Purdue University
Purdue e-Pubs

International Refrigeration and Air Conditioning Conference

School of Mechanical Engineering

2000

Dynamic Characteristics of a R-410A Split Air Conditioning System

M. H. Kim
University of Illinois at Urbana-Champaign

C. W. Bullard
University of Illinois at Urbana-Champaign

Follow this and additional works at: http://docs.lib.purdue.edu/iracc

Kim, M. H. and Bullard, C. W., "Dynamic Characteristics of a R-410A Split Air Conditioning System" (2000). *International Refrigeration and Air Conditioning Conference.* Paper 517.
http://docs.lib.purdue.edu/iracc/517

This document has been made available through Purdue e-Pubs, a service of the Purdue University Libraries. Please contact epubs@purdue.edu for additional information.
Complete proceedings may be acquired in print and on CD-ROM directly from the Ray W. Herrick Laboratories at https://engineering.purdue.edu/Herrick/Events/orderlit.html

DYNAMIC CHARACTERISTICS OF A R410A SPLIT AIR CONDITIONING SYSTEM

Man-Hoe Kim and Clark W. Bullard

Department of Mechanical and Industrial Engineering, University of Illinois at Urbana-Champaign
140 MEB, MC-244, 1206 West Green Street, Urbana, IL 61801

ABSTRACT

This paper presents experimental results on the shut-down and start-up characteristics of a residential split system R410A air-conditioner with a capillary tube. During shut-down, the transient characteristics are evaluated by measuring the high and low side pressures and temperatures of the system. The dynamic behavior of the system after start-up is also investigated, at the high temperature cooling test condition. All experiments are performed in a psychrometric calorimeter. The cooling capacity, power consumption, dehumidification capacity and cycle characteristics after start-up are analyzed. The test results show that cooling capacity after start-up can be expressed as the combination of two exponential functions of time, approaching the cooling capacity of steady state.

INTRODUCTION

Because of environmental and energy efficiency concerns, the air-conditioning industry has been forced to look for alternatives to long-standing fluids such as CFC's and HCFC's and examine new technologies that will allow air-conditioning systems, using the next generation of refrigerants, to be more efficient in their energy consumption than their predecessors [1]. R410A is one of the most attractive potential replacements for residential small air conditioning system. The small residential air conditioner is one of the simplest vapor compression refrigeration systems: composed only of a compressor, a condenser, an evaporator, a capillary tube and related attachments. The steady state characteristics of the R410A system as well as the R22 system are well established. The operation of the residential air conditioner is on-off controlled to a temperature set point to meet the cooling load. This cycling affects the seasonal system performance. Therefore, dynamic behaviors for the R22 system have been studied by many investigators [2-13].

Dhar [2] established a mathematical model for transient characteristics of the vapor compression system and investigated the dynamic behaviors for the system. Murphy et al. [3,4] performed experimental studies on the dynamic characteristics of the 3-ton air conditioning system. They investigated temperature behaviors of the evaporator with time and represented refrigeration capacity (Q) at start-up as function of the transient time (t) with steady state capacity (Q_s) and one time constant (τ=28 sec).

$$Q = Q_s\left[1 - \exp(-t/\tau)\right] \tag{1}$$

Chi and Didion [5] developed a model for dynamic behaviors of a residential heat pump and verified the model using the cooling test results of 4-ton residential heat pump. Tanaka et al. [6] reported dynamic characteristics through the start-up and shut-down tests using residential heat pump with a rotary compressor. They measured refrigerant mass in components including a condenser, an evaporator and an accumulator and suggested some techniques to improve start-up performance. Murphy and Goldschmidt [7] investigated experimentally the start-up and shut-down characteristics for a residential split system air conditioner with a reciprocating compressor. Mulroy and Didion [8] performed a study on refrigeration migration and cycle loss using 3-ton split air conditioning system and they presented the capacity of the system during start-up as function of the time, defined by two time constants

$$Q = Q_s\left[1 - \exp(-t/\tau_1)\right]\left[1 + 4.0\exp(-t/\tau_2)\right] \tag{2}$$

τ_1=3.0 min and τ_2=0.8 min. The first and second terms of right hand side of equation (2) indicate performance degradation due to the thermal masses of the components (e.g. heat exchangers) and refrigerant migration,

respectively. Murphy and Goldschmidt [9,10] developed a dynamic model for a split system air conditioning system and investigated transient characteristics of the system. Belth et al. [11] proposed method for measuring the refrigerant distribution among components of the heat pump during the system operation. They presented changing rate of refrigerant mass in each component during transient operation as both cooling and heating modes. Katipamula [12] developed a model for the analysis of performance degradation during on-off cycling of single speed system and compared it to the experimental results. He also investigated temperature and pressure characteristics of the key cycle points and dehumidification capacity. Wang and Wu [13] performed an experimental study on refrigerant migration and system behaviors during the shut-down and start-up of the vapor compression system with a reciprocating compressor and a capillary tube. They showed that average and peak power consumption of the system during start-up could be reduced by 4% and 9.4 %, respectively, using a valve for preventing refrigerant migration after shut-down.

Jacobsen [14] developed a mathematical model for the dynamic behaviors of the domestic refrigerator and verified it using the experimental results. Rubas and Bullard [15] studied cycle loss of the refrigerator with capillary-suction heat exchanger. Judge and Radermacher [16] performed experimental study on the performance of the transient and steady state of a R407C split air conditioning system. They reported cycle losses of the R407C system for the cooling and heating modes are 23.3 % and 11.3 %, respectively, higher than the R22 system. Burns et al. [17] investigated cycle loss of the R410A split system air conditioner and compared it to a R22 system. However, there is no published data for the dynamic behavior of R410A systems in the open literature.

This study presents dynamic characteristics during shut-down and start-up of a single speed R410A split air conditioning system with a capillary tube as an expansion device. During shut-down, the transient behaviors are evaluated by measuring the high and low side pressures and temperatures of the system. The dynamic characteristics of the system after start-up are also investigated at the high temperature cooling test condition. Cooling capacity, power consumption, dehumidification capacity and cycle characteristics after start-up are reported. The refrigerant properties are calculated using REFPROP [18].

EXPERIMENTS

Test unit

The test unit in the study is a residential split type R410A air conditioner that has a rated cooling capacity of 4.13 kW. The unit is composed of the basic components of a vapor compression system: a rotary compressor, a condenser, a capillary tube, an evaporator and such attachments as accumulator and fans. The basic specifications of the test unit are described in Figure 1 and Table 1. Thirty T-type thermocouples are mounted on the key points of the cycle and six pressure transducers are connected to the pressure taps. Test data are collected using a hybrid recorder and a PC.

Test apparatus

All the tests are performed in a psychrometric calorimeter described in Table 2. It composed of two separate constant temperature and humidity chambers. The temperatures and humidities of the chambers are controlled by the refrigeration units, heaters and humidifiers. The dry and wet bulb temperatures of air entering the test unit are maintained within ±0.1°C except dry bulb temperature of ±0.3°C for the outdoor chamber. The cooling capacity of the test unit is calculated by the air enthalpy method in which dry and wet bulb temperatures of air entering and leaving the unit, and evaporator air flow rate are measured. The test equipment has an accuracy of 3% since an accuracy of air flow rate is ±1% and uncertainty of thermodynamic properties of air is within 0.05%.

Test condition and method

The tests are performed according to the standard high temperature cooling test condition of which the dry and wet bulb temperatures for the indoor and outdoor are 27/19.5°C and 35/24°C, respectively. The test unit is installed in the chambers and the test apparatus is operated over two hours. After the operating conditions of the chambers have reached at the steady state, the test unit is started. Confirming that the operation of the unit has reached steady state, the test data are collected every 20 seconds after the shut-down of the test unit. After equilibrium between the high and low side of the unit is reached, the test unit is run again, the test data are collected every 20 seconds after start-up

of the unit. The same procedures are repeated five times to ensure repeatability of the data.

RESULTS AND DISCUSSION

The test results of the R410A split air conditioner with a capillary tube as an expansion device during shut-down and start-up are depicted in Figures 2-10. Figure 2 shows the characteristics of the suction and discharge pressures and temperatures after shut-down. As shown in the Figure, after shut-down of the system, the equilibrium between the high and low side of the unit was reached in three minutes after the refrigerant moves from high side to low side through the capillary tube. The design of the rotary compressor prevents refrigerant migration through the compressor. The pressure difference between high and low sides of the system decreases steadily for 80 seconds after shut-down of the compressor. The saturation temperature in the condenser falls rapidly after shut-down, below the outdoor ambient, causing the remaining liquid to boil. Then the condenser pressure experiences a sharp discontinuity, causing the saturation temperature to rise to ambient temperature, suggesting that the capillary tube inlet suddenly changed from two phase to vapor only, with a correspondingly sharp drop in mass flow rate. The temperature difference between suction and discharge decreases very slowly, suggesting that the tube temperature influenced strongly by axial conduction from the compressor, which has a very large thermal capacitance. This phenomenon may be due to the refrigerant movement very after shut-down and after then due to heat exchange with environment of which temperature maintains at 35°C. The refrigerant in the suction and discharge is in superheated state because the saturation temperature is lower than environment temperature of 35°C.

Figure 3 presents variation of condenser wall temperatures, and the saturation temperature determined from discharge pressure after shut-down. The condensing temperatures after shut-down decrease quickly as pressures equalize, falling below the temperature of the outdoor air. The resulting heat transfer evaporates the remaining refrigerant. After reaching a minimum at a certain time, refrigerant vapor and condenser wall temperatures then increase and approach the value of the steady state. Figure 4 shows how evaporator wall temperature changes with time after shut-down. Evaporating temperatures increase for about 60 seconds due to the refrigerant migration after shut-down, decrease for awhile, and increase again after 180 seconds. The temperature peak actually approached the indoor ambient air temperature for a short time as pressure equalization was determined by the high side pressure, which exceeded the saturation temperature corresponding to the indoor air. Then the rate of migration decreased after the liquid seal at the capillary tube inlet was broken (the discontinuity in Figure 2); the tubes and refrigerant were apparently cooled by the rest of the evaporator thermal mass. Finally the entire mass approached equilibrium with the indoor air over a long period of time, since evaporator situated in the chamber of which dry and wet bulb temperatures maintained at 27°C and 19.5°C, respectively and it absorbed heat from the environment.

Figures 5-7 depicts temperature and pressure characteristics of the key cycle points of the system at start-up. The suction and discharge pressures reach at the equilibrium after about 90 seconds. The suction pressure decreases rapidly for the first 40 seconds and then increases gradually to reach the value of the steady state, while discharge pressure increases fast for about 80 seconds and then approaches steady state very slowly. The suction and discharge temperatures change with variation of refrigerant pressures, but the suction temperature decreases rapidly at the initial stage after start-up and then increases approaching steady state value, which is affected by the temperature of the relatively massive compressor shell. This can be explained observing the refrigerant state after shut-down; most of refrigerant in the evaporator exists in saturation state after shut-down while a small part of refrigerant exists as superheated state in the condenser [8]. When the compressor is on, low side pressure (including the evaporator) decreases instantly and refrigerant flows to the compressor. At the very initial stage at start-up, refrigerant flow discharged from the compressor is larger than that which can flow as vapor or high quality mixture through the capillary tube. Therefore, refrigerant mass in the condenser increases abruptly, thereby increasing condensing temperature and pressure, while refrigerant is depleted from the evaporator and evaporating temperature and pressure decrease rapidly as expected. After a certain amount time, refrigerant flow through capillary tube balances that discharged from the compressor, and condensing and evaporating pressures and temperatures approached then steady state values.

Figures 8-10 show characteristics of the system performance after start-up. As shown in Figure 8, power consumption increases rapidly for the first 60 seconds after start-up and then approaches the steady state value. However, the cooling capacity and coefficient of performance (COP) increase gradually and reach the steady state value after 15 minutes. The cooling capacity (Q) of the system at start-up can be described using two exponential functions of time with two time constants as

$$Q = Q_s[1 - \exp(-t/s_1)]/[1 + 53.48\exp(-t/s_2)] \quad (3)$$

Where Q_s is steady state cooling capacity and time constants s_1 and s_2 are 2.45 and 0.34 min, respectively. Equation (3) is similar to equation (2) which Mulroy and Didion [8] extracted from their study. However, they expressed cooling capacity as a product of two exponential functions. The difference between two equations may be partly due to the fact that they did not consider decreasing of the cooling capacity due to the latent heat, and the fact that different test units were used for each study. The COP of the system at start-up also can be approximated as exponential functions of time with the steady state COP_s and two time constants

$$COP = COP_s[1 - \exp(-t/c_1)]/[1 + 48.63\exp(-t/c_2)] \quad (4)$$

Where time constants c_1 and c_2 are 2.27 and 0.35 min, respectively. The cooling capacity and COP of the system at start-up can approximate the measured cooling capacity and COP within 3% accuracy as shown in Figure 8.

Figure 9 presents the cooling capacity with sensible and latent heats. It was observed that total cooling capacity increases very slowly due to negative latent heat at the initial stage after start-up. This may be explained observing the dehumidification capacity after start-up as shown in Figure 10. Some condensate remains on the evaporator from the previous on-cycle, and the fin surfaces are initially warm. Figure 7 shows that it takes more than a minute before all the tubes are colder than the dew point, and probably larger for the fins. During that period, condensate evaporates from the surface, resulting in the negative latent heat shown in Figure 9-10. Eventually the rate of condensation (on the coldest parts) exceeds the evaporation from the warmer parts, and the latent heat transfer rate reaches steady state after about three minutes. Performance degradation of the system after start-up is attributed mainly to the shortfall in sensible heat transfer, except during the first three minutes when latent heat transfer is negative or small. Overall, most of this performance degradation is due to the refrigeration migration during shut-down and the thermal masses of the basic components such as heat exchangers.

Figure 10 depicts dehumidification capacity and air flow rate of the indoor unit. Dehumidification capacity increases rapidly for 3 minutes except the first 70 seconds when humidification process occurs, and approaches the steady state value. The air flow rate of the indoor unit increases gradually with time. The low air flow after start-up is probably attributable to the apparatus. The measuring device for air flow rate of the indoor unit has an auxiliary fan to regulate the pressure at the outlet of indoor unit to equal the atmospheric pressure, and it takes time to achieve the balance.

CONCLUDING REMARKS

An experimental study on the dynamic characteristics has been performed using a R410A residential split air conditioner with a capillary tube as an expansion device. A series of tests were carried out in the psychrometric calorimeter based on the standard high temperature cooling test condition and the following conclusions are obtained.

1. The pressure of the system after shut-down reaches at equilibrium within three minutes and increases gradually due to heat exchange with environment before reaching to the pressure of steady state.

2. The refrigerant in the evaporator exists in saturated state while the refrigerant in the condenser is at superheated state after shut-down.

3. The performance degradation of the system is largely due to latent heat for 70 seconds after start-up, since condensation water on the evaporator surface is released to environment.

4. The cooling capacity and COP of the system after start-up can be expressed within 3% accuracy as a quotient of two exponential functions of time with two time constants; the system reaches steady state in about 15 minutes.

5. The performance degradation after start-up may be attributed to the refrigeration migration during shut-down and the thermal masses of the components such as heat exchangers.

ACKNOWLEDGEMENTS

We are grateful for support of this study to Samsung Electronics Co., Ltd. and the 25 member companies of the Air Conditioning and Refrigeration Center (ACRC) at the University of Illinois at Urbana-Champaign.

REFERENCES

(1) Kirkwood, A.C. and Bullard, C.W., 1999, "Modeling, design, and testing of a microchannel split-system air conditioner," ACRC Technical Report TR-149, University of Illinois at Urbana-Champaign.
(2) Dhar, M., 1978, "Transient analysis of refrigerating system, Ph.D. Thesis," Purdue University.
(3) Murphy, W.E. and Goldschmidt, V.W., 1979, "The degradation coefficient of a field tested self-contained 3-ton air-conditioner," ASHRAE Trans., Vol.85, Pt.2, pp. 396-405.
(4) Goldschmidt, V.W., Hart, G.H. and Reiner, R.C., 1980, "A note on the transient performance and degradation coefficient of a field tested heat pump- cooling mode," ASHRAE Trans., Vol.86, Pt.2, pp.368-375.
(5) Chi, J. and Didion, D.A., 1982, "A simulation of transient performance of heat pump," Int. J. of Refrig., Vol.5, No.3, pp.176-184.
(6) Tanaka, N., Ikekuchi, M. and Yamanaka, G., 1982, "Experimental study on the dynamic characteristics of a heat pump," ASHRAE Trans., Vol.88, Pt.2, pp.323-331.
(7) Murphy, W.E. and Goldschmidt, V.W., 1984, "Transient response of air-conditioners-a qualitative interpretation through a sample case," ASHRAE Trans., Vol.90, Pt.1B, pp.997-1008.
(8) Mulroy, W.J. and Didion, D.A., 1985, "Refrigerant migration in a split-unit air-conditioner," ASHRAE Trans., Vol.91, Pt.1A, pp.193-206.
(9) Murphy, W.E. and Goldschmidt, V.W., 1985, "Cyclic characteristics of a residential air-conditioner - modeling of start-up transient," ASHRAE Trans., Vol.91, Pt.2A, pp.427-444.
(10) Murphy, W.E. and Goldschmidt, V.W., 1986, "Cyclic characteristics of a residential air-conditioner - Modeling of shutdown transient," ASHRAE Trans., Vol.92, Pt.1A, pp.186-202.
(11) Belth, M.L., Grzymala, T.E. and Tree, D.R., 1988, "Transient mass flow rate of a residential air-to-air heat pump," Int. J. of Refrig., Vol.11, pp.298-304.
(12) Katipamula, S., 1989, "A study of the transient behavior during start-up of residential heat pumps," Ph.D. Thesis, Texas A&M University.
(13) Wang, J. and Wu, Y., 1990, "Start-up and shut-down operation in a reciprocating compressor refrigeration system with capillary tubes," Int. J. of Refrig., Vol.13, pp.187-190.
(14) Jakobsen, A., 1995, "Energy Optimization of Refrigeration Systems: The Domestic Refrigerator - a Case Study," Ph.D. Thesis, The Technical University of Denmark, pp.77-83.
(15) Rubas, P.J. and Bullard, C.W., 1995, "Factors contributing to refrigerator cycling losses," Int. J. of Refrig., Vol.18, No.3, pp.168-176.
(16) Judge, J.F. and Radermacher, R., 1995, "The transient and steady state performance of R-22 and R-407C," Heat Pump and Refrigeration Systems Design, Analysis and Applications, ASME, AES-Vol. 34, pp.1-9.
(17) Burns, L.D., Hoffman, L. and Schuster, D., 1996, "R-410A experiences in unitary air conditioner systems," The International Symposium on HCFC Alternative Refrigerants, The Japan Refrigeration and Air Conditioning Industry Association, Kobe, Japan, pp.61-66.
(18) Huber, M., Gallagher, J., McLinden, M. and Morrison, G., 1996, "NIST Thermodynamic Properties of Refrigerants and Refrigerant Mixtures Database (REFPROP)," Version 5.0, NIST.

Table 1 Specifications of the test unit

Items	Specifications
Rated cooling capacity	4.13 kW
Refrigerant/oil	R410A/POE (VG68)
Compressor	Rotary vane type
Evaporator (height x width)	ϕ7.0 mm, 2-row 12 tubes (252x719 mm)
Condenser (height x width)	ϕ9.52 mm, 1-row 28 tubes (700x690 mm)
Expansion device	Capillary (ϕ1.7 mm, L=800 mm)
Indoor fan	Cross flow fan (ϕ95.5 mm, L=734 mm)
Outdoor fan	Propeller fan (ϕ400 mm, L=96mm)

Table 2 Specifications of the psychrometric calorimeter

Items		Specifications
Available test ranges	Cooling capacity (kW)	1.16 - 11.63
	Heating capacity (kW)	1.75 - 13.96
	Indoor air flow rate (m^3/min)	4 - 40
	Temperature and humidity	10-40 °C, 30-85 %(indoor), -15-55 °C, 30-95 %(outdoor)
Cooling unit (kW)		2 x 4.0 (indoor), 2 x 5.5 (outdoor)
Heater (kW)		24 (indoor), 30 (outdoor)
Humidifier (liter/h)		Max. 7.5 (indoor), Max. 4.5 (outdoor)
Cooling tower (RT)		40

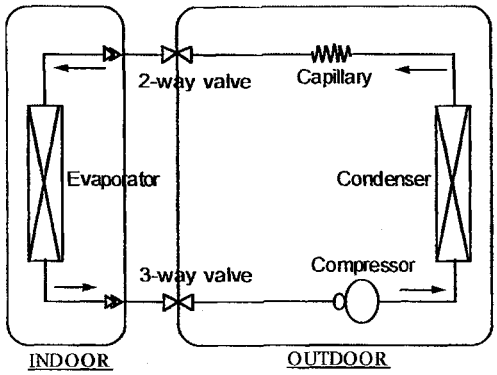

Figure 1. Schematic diagram of the test unit

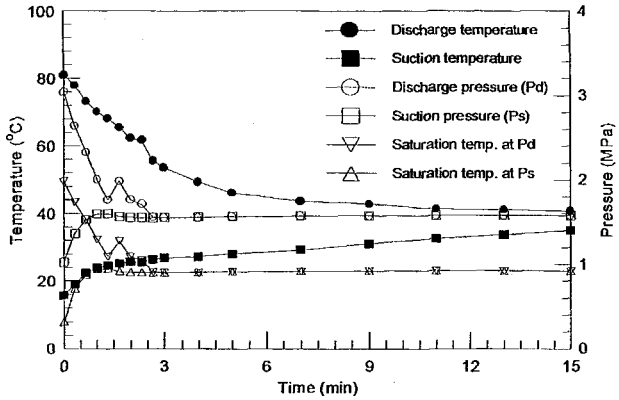

Figure 2. Suction and discharge temperatures and pressures during shut-down

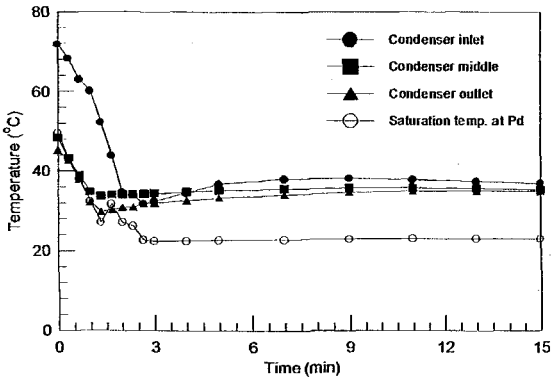

Figure 3. Condenser wall temperatures during shut-down

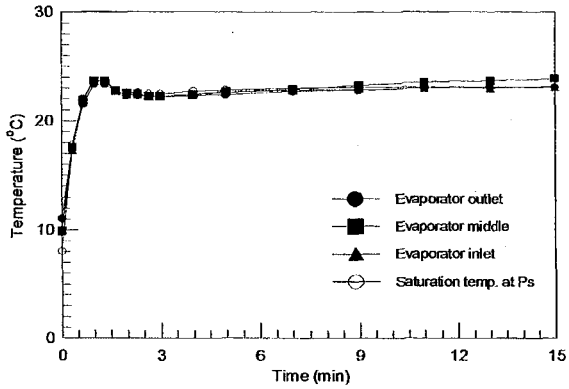

Figure 4. Evaporator wall temperatures during shut-down

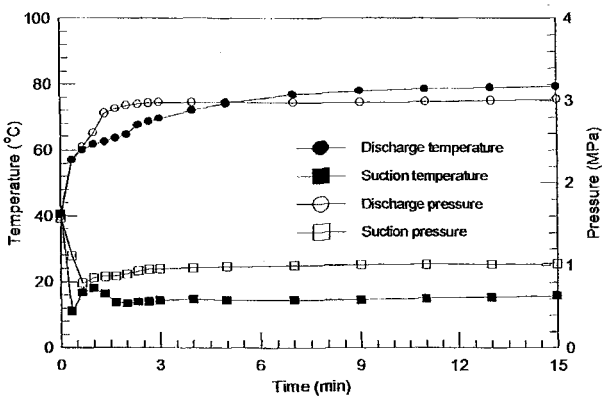

Figure 5. Suction and discharge temperatures and pressures at start-up

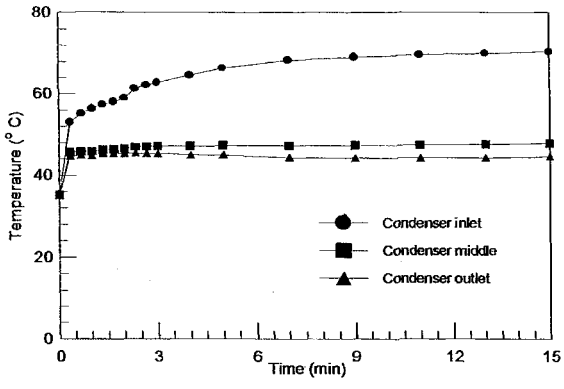

Figure 6. Condenser wall temperatures at start-up

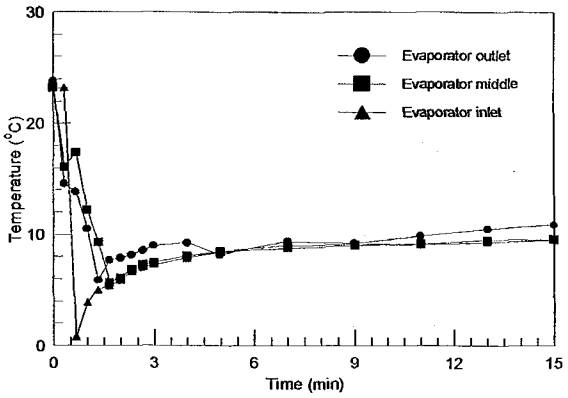

Figure 7. Evaporator wall temperatures at start-up

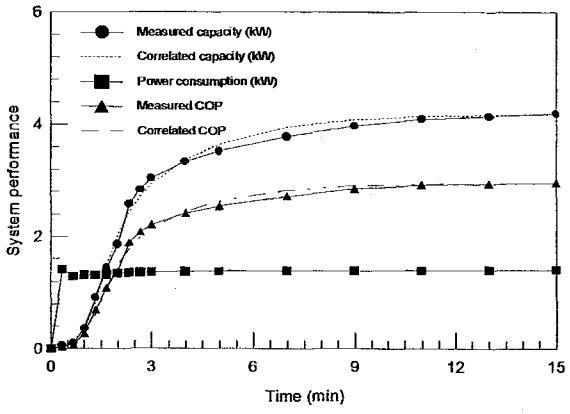

Figure 8. System performance at start-up

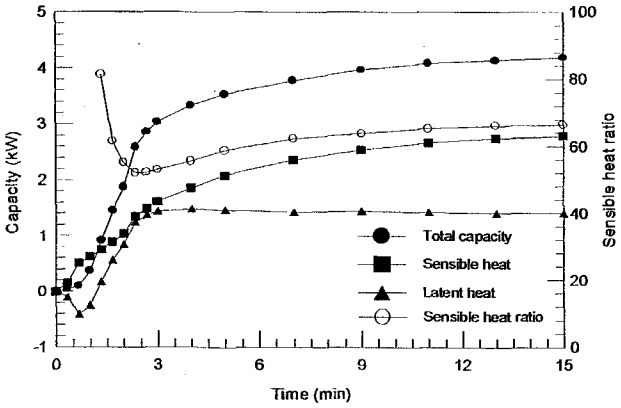

Figure 9. Cooling capacity at start-up

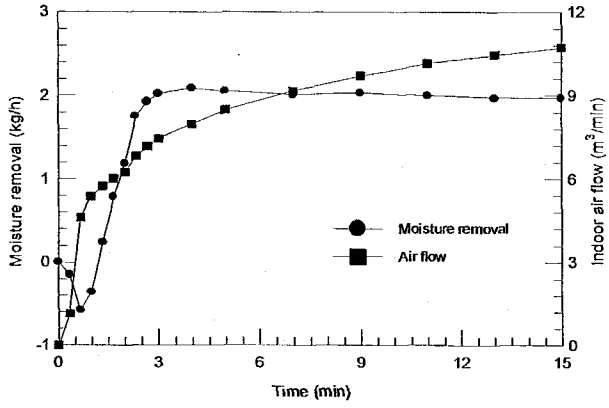

Figure 10. Moisture removal and indoor air flow rate at start-up